COMPRESSIVE SENSING IN THROUGH-THE-WALL RADAR IMAGING

Michael Leigsnering, Christian Debes and Abdelhak M. Zoubir

Signal Processing Group
Technische Universität Darmstadt
Darmstadt, Germany

ABSTRACT

High resolution through-the-wall radar imaging (TTWRI) demands wideband signals and large array apertures. Thus a vast amount of measurements is needed for a detailed reconstruction of the scene of interest. For practical TTWRI systems it is imperative to reduce the number of samples to cut down on hardware cost and/or acquisition time. This can be achieved by employing compressive sensing (CS). Existing approaches imply a point target assumption, which may not hold in practical applications. We apply a novel CS approach for TTWRI using the 2D discrete wavelet transform to sparsify images. In this fashion, we overcome the above stated limitation and are able to deal with extended targets. Experimental results show that high image qualities are obtained, similar to images generated using the full measurement set.

Index Terms— Through-the-wall, radar imaging, compressive sensing, wavelets

1. INTRODUCTION

Through-the-wall radar imaging (TTWRI) is of high practical interest for many civil, law enforcement and military applications [1, 2, 3]. The ultimate goal of TTWRI is to acquire detailed information of a scene using electromagnetic wave propagation that cannot be observed by other means. Hence high-resolution 3D images of the scene behind walls or visually opaque obstacles are desired.

High crossrange and downrange resolution calls for wideband large aperture systems. TTWRI systems either use physical or synthetic aperture arrays employing direct wideband pulse formation or a stepped-frequency approach. This results in either a large number of costly physical sensors or a long acquisition time when placing a single sensor at various positions. Thus, it is desirable to reduce the number of necessary array elements to cut down on hardware cost and/or recording time.

Compressive sensing (CS) can be used to achieve the desired reduction of data samples [4, 5, 6]. CS aims at recovering a signal from significantly less measurements than required by Shannon's sampling theorem. An important prerequisite is that the signal is sparse or can be sparsely expressed in a known basis. The measurements are obtained by linearly correlating the signal with a fixed set of waveforms. Using a non-linear program, the original signal can be reconstructed.

In TTWRI, the desired image vector ($\boldsymbol{s}$) can be reconstructed from a reduced number of measurements ($\boldsymbol{y}$). The work in [5, 6] assumes that the reconstructed image of the scene itself is sparse, which holds only for the case of point targets. In our work, we overcome this limitation by using the 2D discrete wavelet transform (DWT) as a sparse basis for the image of the scene.

For assessing the proposed approach we used a synthetic aperture, stepped-frequency setup. Both the number of array elements and frequency bins can be reduced significantly, resulting in an overall reduction of measurements by up to 98 %. The desired image of the scene is directly obtained as the optimization result of the compressive sensing algorithm. Due to the high SNR in CS results, the image can be segmented very efficiently by simple thresholding.

In Sections 2 and 3, we discuss the basic equations for TTWRI and revisit briefly the fundamentals of CS theory, respectively. In Section 4 we derive the proposed CS beamforming algorithm. Section 5 provides an assessment of the performance using experimental data recorded in a TTWRI lab.

2. THROUGH-THE-WALL RADAR IMAGING

The propagation of electromagnetic waves from a transmitter to the target and back to a receiver is subject to distortions. On the way to the target the wave is refracted twice (on the air-wall and the wall-air interface). It is reflected by a possible target and again double refracted on the way to the receiver. The wave propagation is modeled for subsequently deriving the image formation algorithm.

In the following we consider wideband delay and sum beamforming (DSBF) for TTWRI as proposed in [2]. The proposed CS techniques can, however, be applied to various imaging techniques in TTWRI.

2.1. Received signal model

Aiming for a high downrange resolution, a wideband pulse must be used [2]. Assume that the wideband transceivers are placed on a physical or synthetic aperture array consisting of N elements. In the stepped frequency approach the pulse is approximated by transmitting narrowband signals at discrete frequencies. Thus a finite number M of monochromatic signals with regular spaced frequencies f_m are used, covering the desired band, where $m = 0, 1, \ldots, M-1$.

The received signal model assumes that the region of interest can be described by P discrete targets with different reflectivities. Now the signal $y[m, n]$ at array element n and frequency f_m can be expressed as

$$y[m, n] = \sum_{p=0}^{P-1} \sigma_p S(\omega_m) \exp(-j2\pi f_m \tau_{pn}), \qquad (1)$$

where $S(\omega_m)$ is the weight of the m-th frequency, σ_p denotes the reflectivity of the p-th target and $n = 0, 1, \ldots, N-1$. If the wall parameters, i.e. the thickness and the permittivity, were known, the round-trip delay between the p-th target and the n-th receiver τ_{pn} can be calculated from geometric considerations. For the derivation of the delay for monostatic radar, see [2].

2.2. Delay and sum beamforming

The target region can be divided into a regular grid with finite number of pixels. Suppose the region of interest covers N_x and N_y points in crossrange and downrange, respectively. Using an appropriate numbering scheme, a single index q is sufficient for addressing all $N_x N_y$ grid points (x_q, y_q), where $q = 0, 1, \ldots, N_x N_y - 1$.

By applying conventional DSBF, the beam can be steered at each pixel (x_q, y_q). The complex-valued image or B-scan can be obtained by [2]

$$I(x_q, y_q) = \frac{1}{MN} \sum_{n=0}^{N-1} \sum_{m=0}^{M-1} y[m, n] \exp(j2\pi f_m \tau_{qn}), \qquad (2)$$

where τ_{qn} is the delay compensation for the n-th receiver steering the beam at position (x_q, y_q), M is the number of frequency bins and N is the number of array elements. It is noteworthy that the above equation employs wideband, near-field beamforming. Thus, the frequency dependent term cannot be factored out of the exponential and the function for the propagation delay τ_{qn} is highly non-linear.

3. COMPRESSIVE SENSING

Let $\boldsymbol{x}$ be a sparse representation of the signal vector $\boldsymbol{s}$, related by an orthonormal transformation

$$\boldsymbol{s} = \boldsymbol{\Psi x}. \qquad (3)$$

Furthermore, the linear measurement equation can be expressed as $\boldsymbol{y} = \boldsymbol{A s}$, where $\boldsymbol{A}$ is the so-called measurement matrix and $\boldsymbol{y}$ is the vector of measurements. If there is a sparse basis for the vector of interest $\boldsymbol{s}$, CS theory [7] states that it can be recovered with good accuracy from only few measurements by the convex program

$$\boldsymbol{x}^* = \arg\min_{\boldsymbol{x}} \|\boldsymbol{x}\|_1 \quad \text{s.t.} \quad \boldsymbol{y} = \boldsymbol{A\Psi x}, \qquad (4)$$

where $\|\cdot\|_1$ is the ℓ_1 norm. Equation (3) can be used to recover the signal of interest.

If additive white Gaussian noise is taken into account, (4) is modified to [8]

$$\boldsymbol{x}^* = \arg\min_{\boldsymbol{x}} \frac{1}{2} \|\boldsymbol{A\Psi x} - \boldsymbol{y}\|_2^2 + \tau \|\boldsymbol{x}\|_1, \qquad (5)$$

where the positive parameter τ trades off between sparsity of the solution and residuals of the measurement equation.

4. COMPRESSIVE SENSING IN THROUGH-THE-WALL RADAR IMAGING

The measurements in Equation (1) can be vectorized for notational convenience. The measured data vector $\boldsymbol{y} \in \mathbb{C}^{MN \times 1}$ is obtained by stacking all $M \cdot N$ measurements $y[m, n]$ in one column vector.

$$\boldsymbol{y} = [y[0, 0], \ldots, y[M-1, 0], \ldots, y[M-1, N-1]]^T$$

The complex reflectivities σ_p corresponding to targets at positions (x_p, y_p) can be vectorized as $\boldsymbol{s} = [\sigma_1, \sigma_2, \ldots, \sigma_{P-1}]^T$.

Now (1) can be rewritten as

$$\boldsymbol{y} = \boldsymbol{\Phi s}, \qquad (6)$$

where $\boldsymbol{\Phi} \in \mathbb{C}^{MN \times P}$ is the so called overcomplete measurement dictionary, whose elements are defined by

$$[\boldsymbol{\Phi}]_{ip} = \exp(-j2\pi f_m \tau_{pn}), \quad m = i \bmod M, \quad n = \lfloor i/M \rfloor, \quad i = 0, 1, \ldots, MN-1.$$

Alternatively the target reflectivity vector $\boldsymbol{s}$ can be seen as a weighted indicator function,

$$[\boldsymbol{s}]_p = \begin{cases} \sigma_p & \text{if a target is present at } (x_p, y_p), \\ 0 & \text{if no target is present at } (x_p, y_p). \end{cases} \qquad (7)$$

If the points (x_p, y_p) are sampled on the same grid as (x_q, y_q) the vector $\boldsymbol{s}$ corresponds to the image $I(x_q, y_q)$. Hence (6) relates the desired B-scan image to the measurements $\boldsymbol{y}$.

4.1. Sparse B-scan CS Beamforming

The existing approaches for CS in TTWRI as proposed in [5, 6] assume that the complex image $\boldsymbol{s}$ itself is sparse. In the

case of few point targets $P \ll N_x N_y$ in the region of interest, this assumption holds with reasonable accuracy. The basis vectors of the sparse basis simply form an identity matrix, $\boldsymbol{\Psi} = \boldsymbol{I}$ with size $N_x N_y$.

As the goal is to reduce the number of measurements, only a subset of the full measurement vector is used. Let k_j be a random sampling index with $k_j \in [0, 1, \ldots, MN-1]$ and $j = 0, 1, \ldots, J-1$, where $J \ll MN$ holds. The B-scan image can now be recovered by applying (5)

$$\hat{\boldsymbol{s}} = \arg\min_{\boldsymbol{s}} \frac{1}{2}\|\bar{\boldsymbol{y}} - \boldsymbol{A}\boldsymbol{s}\|_2^2 + \tau\|\boldsymbol{s}\|_1, \tag{8}$$

where

$$[\bar{\boldsymbol{y}}]_j = [\boldsymbol{y}]_{k_j} \quad [\boldsymbol{A}]_{jp} = [\boldsymbol{\Phi}]_{k_j p}.$$

It is beneficial if k_j is not chosen totally at random. Huang et al. proposed in [5] choosing a random subset of the array elements and frequency bins respectively. The array elements and frequency subset should cover the whole aperture and frequency band. Subsequently measurements at all array element / frequency pairs from the two subsets are taken. By exploiting this structure the total amount of needed frequencies and array elements can be reduced.

4.2. CS Beamforming using DWT

We aim for a new CS approach in TTWRI overcoming the point target limitation in existing work [5, 6]. In practical high-resolution TTWRI systems the point target assumption does not hold, as even medium sized targets (e.g. humans) appear extended rather than point-like in B-scans. Furthermore, for a subsequent classification of the targets, the information of the shape of the targets needs to be preserved. Hence, a more sophisticated sparse basis for the application of CS in TTWRI is desired for taking extended targets into account.

The 2D DWT is commonly used as a sparsifying transform for CS imaging [9]. There are numerous applications for 2D wavelet bases in CS imaging, e.g. medical magnetic resonance imaging (MRI) [10] or radar imaging [4]. Thus, we combine the CS approach in Equation (8) with the 2D DWT yielding a novel approach for CS in TTWRI.

Let $\boldsymbol{\Psi}$ be the matrix spanning the vector space of the wavelet basis and $\boldsymbol{x}$ be the vector of wavelet coefficients. Now the B-scan vector $\boldsymbol{s}$ can be expressed by Equation (3). Combining equations (8) and (3) yields the convex program

$$\hat{\boldsymbol{x}} = \arg\min_{\boldsymbol{x}} \frac{1}{2}\|\bar{\boldsymbol{y}} - \boldsymbol{A}\boldsymbol{\Psi}\boldsymbol{x}\|_2^2 + \tau\|\boldsymbol{x}\|_1. \tag{9}$$

It should be emphasized that (9) promotes sparsity of the vector of wavelet coefficients $\boldsymbol{x}$, rather than sparsity of the B-scan itself. The optimization result for the B-scan $\hat{\boldsymbol{s}}$ can be obtained through (3).

We carried out an extensive study of the performance of different 2D DWTs in the proposed CS algorithm. The DWT using Daubechies, Coiflet and Biorthogonal wavelets [9] as well as the dual-tree complex wavelet transform (DT-CWT) [11] were applied in the CS approach. The reconstruction quality of the B-scan was assessed using the above stated wavelet families at different orders.

We deem the DT-CWT as the best candidate for TTWRI images, as its results show the fewest artifacts and a smooth appearance, possibly due to the good directional selectivity and approximate shift invariance of the DT-CWT [11].

5. EXPERIMENTAL RESULTS

The measurements were acquired using a TTWRI system in an anechoic chamber with a reflective floor. A uniform linear array with 57 elements with a spacing of 2.2 cm is placed in front of a concrete wall at a distance of 1.05 m. From each element 801 monofrequent measurements are taken equally spaced from 700 MHz to 3.1 GHz. The center of the array is 1.22 m above the floor. The wall parameters, wall thickness $d = 14.3$ cm and relative permittivity $\epsilon = 7.6632$, are known. Behind the wall a single standing human in 2.5 m distance is facing the wall.

In order to quantify the necessary amount of data, the influence of the number of measurements on the image quality was evaluated. The percentage of considered data records ranges from 5% to 50% of both, frequency bins and array elements. The images reconstructed from partial and full measurement data, respectively, were compared using the structural similarity (SSIM) index [12]. This quality metric is used in image processing for comparing two images, e.g. the original and a distorted version. The SSIM yields a value smaller or equal to 1, where 1 means the two images are matching perfectly. The similarity of structural features in the image, rather than absolute pixel values are assessed. Thus SSIM is more suitable for evaluating the reconstruction. The SSIM value for each point in the graph was averaged over 5 realization and is depicted in Figure 1.

It can be observed that the image quality increases with the number of array elements and frequency bins respectively. There is a trade-off behavior for those two parameters: If the number of frequencies bins is decreased the number of array elements has to be increased (and vice versa) to keep the image quality constant. The typical thresholding behavior of the compressive sensing approach can be observed. If the number of measurements gets below a certain threshold the image quality drops rapidly.

An image of the considered scene is shown in Figure 2d. The proposed approach (using DT-CWT) is compared to the existing CS beamforming algorithm and conventional DSBF. In Fig. 2a, the target and the shadow (ghost target due to multipath propagation via the reflective floor) is clearly resolved whereas the recovered image in Fig. 2b is hard to read. The image formed by DSBF using full measurements is shown for comparison in Figure 2b. All B-scans are normalized to their own maximum and shown on the same 60 dB scale.

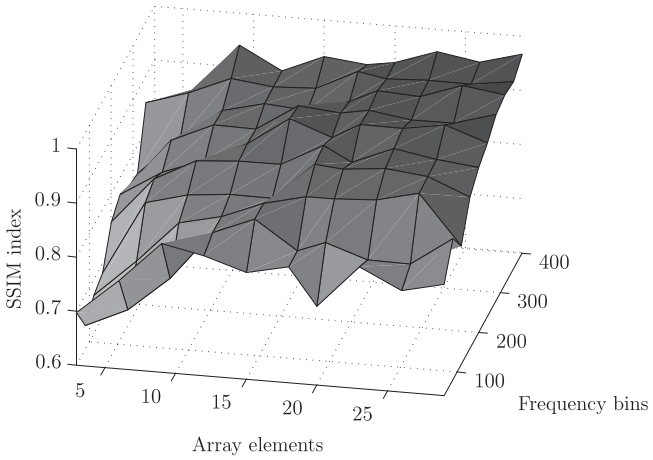

Fig. 1: SSIM metric versus number of array elements and frequency bins

6. CONCLUSIONS

A novel approach for the application of CS in TTWRI based on the DWT has been presented. By employing the DWT as sparsifying transform, this approach is suitable for correctly representing large targets in high resolution imaging. It has been successfully evaluated using experimental data and improves the image quality compared to existing CS beamforming algorithms.

ACKNOWLEDGEMENT

The authors would like to thank Prof. Dr. Moeness Amin and Dr. Fauzia Ahmad from the Center of Advanced Communications at Villanova University, Villanova, PA, USA, for providing the experimental data.

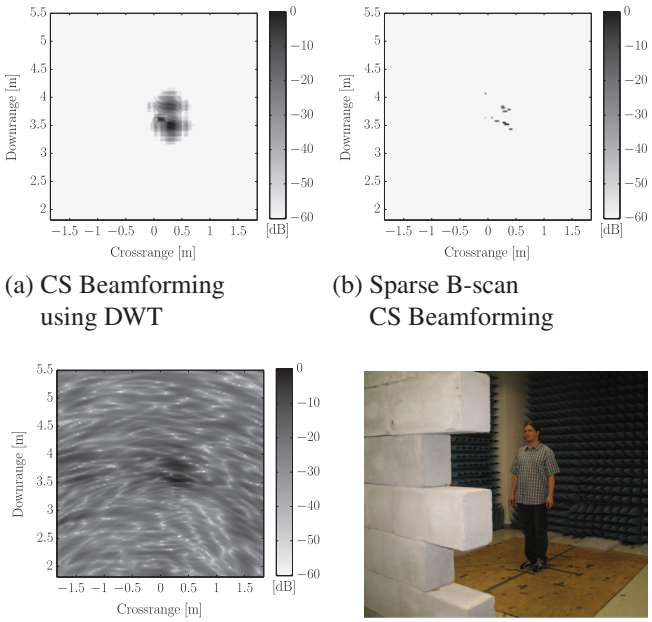

(a) CS Beamforming using DWT

(b) Sparse B-scan CS Beamforming

(c) Conventional DSBF

(d) Human facing the wall

Fig. 2: Images (a) - (c) show B-scans of the scene in (d) applying different beamforming algorithms. One fourth of the array elements and frequency bins were used for the formation of (a) and (b). Image (c) was created using the full set of measurements.

7. REFERENCES

[1] M.G. Amin, Ed., *Through-the-Wall Radar Imaging*, CRC Press, 2010.

[2] F. Ahmad and M.G. Amin, "Multi-location wideband synthetic aperture imaging for urban sensing applications," *Journal of the Franklin Institute*, vol. 345, no. 6, pp. 618 – 639, 2008.

[3] C. Debes, M.G. Amin, and A.M. Zoubir, "Target detection in single- and multiple-view through-the-wall radar imaging," *IEEE Transactions on Geoscience and Remote Sensing*, vol. 47, no. 5, pp. 1349–1361, 2009.

[4] R. Baraniuk and P. Steeghs, "Compressive radar imaging," in *IEEE Radar Conference*, april 2007, pp. 128 –133.

[5] Q. Huang, L. Qu, B. Wu, and G. Fang, "UWB through-wall imaging based on compressive sensing," *IEEE Transactions on Geoscience and Remote Sensing*, vol. 48, no. 3, pp. 1408 –1415, 2010.

[6] Y.-S. Yoon and M.G. Amin, "Compressed sensing technique for high-resolution radar imaging," in *Proceedings of SPIE*, 2008, vol. 6968, p. 69681A.

[7] E.J. Candès, J.K. Romberg, and T. Tao, "Stable signal recovery from incomplete and inaccurate measurements," *Communications on Pure and Applied Mathematics*, vol. 59, no. 8, pp. 1207, 2006.

[8] M.A.T. Figueiredo, R.D. Nowak, and S.J. Wright, "Gradient projection for sparse reconstruction: Application to compressed sensing and other inverse problems," *IEEE Journal of Selected Topics in Signal Processing*, vol. 1, no. 4, pp. 586 –597, dec. 2007.

[9] S. Mallat, *A Wavelet Tour of Signal Processing, Third Edition: The Sparse Way*, Academic Press, 3 edition, December 2008.

[10] M. Lustig, D. Donoho, and J.M. Pauly, "Sparse MRI: The application of compressed sensing for rapid MR imaging," *Magnetic Resonance in Medicine*, vol. 58, pp. 1182–1195, 2007.

[11] N.G. Kingsbury, "Image processing with complex wavelets," *Phil. Trans. Royal Society London A*, vol. 357, pp. 2543–2560, 1997.

[12] Z. Wang, A.C. Bovik, H.R. Sheikh, and E.P. Simoncelli, "Image quality assessment: from error visibility to structural similarity," *IEEE Transactions on Image Processing*, vol. 13, no. 4, pp. 600–612, 2004.